Petroleum Science 20 (2023) 3598–3609

Contents lists available at ScienceDirect

Petroleum Science

journal homepage: www.keaipublishing.com/en/journals/petroleum-science

Original Paper

Experimental study on the degree and damage-control mechanisms of fuzzy-ball-induced damage in single and multi-layer commingled tight reservoirs

Chinedu J. Okere [a, b, *], James J. Sheng [a, b], Li-Kun Fan [c], Xiao-Wei Huang [d], Li-Hui Zheng [b, **], Pan-Feng Wei [d]

[a] Bob L. Herd Department of Petroleum Engineering, Texas Tech University, TX, USA
[b] College of Petroleum Engineering, China University of Petroleum (Beijing), Beijing, 102249, China
[c] China Changqing Oilfield Company, CNPC, Xi'an, 710018, Shaanxi, China
[d] Beijing LihuiLab Energy Technology Co., Ltd., Beijing, 102200, China

ARTICLE INFO

Article history:
Received 14 September 2022
Received in revised form
6 January 2023
Accepted 23 May 2023
Available online 23 May 2023

Edited by Jia-Jia Fei

Keywords:
Drilling
Fracture
Fuzzy-ball fluids
Formation damage analysis
Muti-layer tight reservoirs
Permeability damage index
Flow rate damage index

ABSTRACT

Fuzzy-ball working fluids (FBWFs) have been successfully applied in different development phases of tight reservoirs. Field reports revealed that FBWFs satisfactorily met all the operational and reservoir damage control requirements during their application. However, the damage-control mechanisms and degree of formation damage caused by fuzzy-ball fluids have not been investigated in lab-scale studies so far. In this study, the degree of fuzzy-ball-induced damage in single-and double-layer reservoirs was evaluated through core flooding experiments that were based on permeability and flow rate indexes. Additionally, its damage mechanisms were observed via scanning electron microscope and energy-dispersive spectroscopy tests. The results show that: (1) For single-layer reservoirs, the FBWF induced weak damage on coals and medium-to-weak damage on sandstones, and the difference of the damage in permeability or flow rate index on coals and sandstones is below 1%. Moreover, the minimum permeability recovery rate was above 66%. (2) For double-layer commingled reservoirs, the flow rate index revealed weak damage and the overall damage in double-layer was lower than the single-layer reservoirs. (3) There is no significant alteration in the microscopic structure of fuzzy-ball saturated cores with no evidence of fines migration. The dissolution of lead and sulfur occurred in coal samples, while tellurium in sandstone, aluminum, and magnesium in carbonate. However, the precipitation of aluminum, magnesium, and sodium occurred in sandstone but no precipitates found in coal and carbonate. The temporal plugging and dispersion characteristics of the FBWFs enable the generation of reservoir protection layers that will minimize formation damage due to solid and fluid invasion.

1. Introduction

Formation damage is an undesirable problem that occurs during several development stages of petroleum reservoirs and results in significant productivity loss. Studies have shown that the major causes of formation damage due to the injection of foreign fluids that leads to adverse rock-fluid interactions, clogging of the pore systems by migrating particles, and the mechanical distortion of the rock matrix at a constant action of stress and fluid shear (Civan, 2007; Halim et al., 2021; Liang et al., 2017; Yang et al., 2013). Due to the inefficacy of reservoir engineers in obtaining exact samples and performing detailed measurements on the desired region and location of the reservoir, it is usually difficult to quantify working fluid-induced damage. Over the years, several techniques for quantifying formation damage have been developed by deploying accessible data to obtain the type, range, and degree of damage. These techniques are generally classified into fields (well logging, well testing, analysis of production performance, core and fluid

* Corresponding author. Bob L. Herd Department of Petroleum Engineering, Texas Tech University, TX, USA.
** Corresponding author.
E-mail addresses: chitex41@yahoo.com (C.J. Okere), 13911605104@139.com (L.-H. Zheng).

https://doi.org/10.1016/j.petsci.2023.05.017

analysis data) and laboratory techniques (steady and unsteady state methods) (Okere et al., 2020). In addition, research on the degree and mechanisms of working fluid damage have been extensively studied by previous scholars.

To mention a few related research that was based on theoretical and field-scale evaluation of working fluid damage models, Kumar and Todd (1988) proposed a mathematical model for predicting reservoir damage caused by the encroachment of clay particles. Sui and Zhu (2012) developed a wellbore and reservoir coupled flow model for multilayer commingled gas reservoirs including both damaged and non-Darcy skin in each commingled layer. This study made the first theoretical attempt to evaluate formation damage in multi-layer commingled reservoirs. Huang et al. (2017) used a new well interpretation model to estimate formation damage and fracture closure in tight gas reservoirs. Larestani et al. (2022) established machine learning-based models for forecasting permeability damage during waterflooding operations. These theoretical models are time-saving and may enhance the understanding of a system, however, based on the ideal assumptions made during the derivation of the models, they cannot precisely evaluate working fluid damage (Bai, 2019; Tao et al., 2022; Wang et al., 2018).

On the other hand, some scholars have recently made significant efforts to experimentally quantify working fluid damage in single and multi-layer reservoirs. Byrne et al. (2000) performed experiments such as core flooding, scanning electron microscope (SEM), and thin section analyses to determine the damage mechanisms such as solid invasion, solid particle precipitation, and fines migration. Wang et al. (2019) and Dang et al. (2022) studied materials and the mechanisms of formation damage in tight gas reservoirs via several dynamic filtration experiments and SEM/EDS tests. Ding et al. (2019) proposed a new experimental platform for evaluating formation damage caused by water and gas back-flow behavior during commingled production in multilayer tight gas reservoirs. Okere et al. (2020) analyzed six general laboratory permeability test methods using experimental rankings, statistical algorithms, and a theoretical approach. All previous experimental studies on formation damage evaluation were based on permeability index and most of them focused on single-layer reservoir systems. In 2022, an evaluation index was proposed for the estimation of working fluid damage in single and multi-layered reservoirs (Liu et al., 2022). However, the analysis performed in the study utilized simulated working fluids which could provide unrealistic conclusions. More so, the feasibility of the instantaneous flow rate index especially with an established working fluid needs to be further verified. Given the scarcity of research on the experimental evaluation of working fluid-induced damage in multi-layer reservoirs and the shortcomings of previous publications, it is significant to conduct a flow rate-based multi-layer reservoir damage evaluation experiment using an established working fluid.

The fuzzy-ball working fluid (FBWF) invented by Zheng et al. (2012) is an established working fluid that has been reportedly applied to over 1000 wells across the globe. Experimental and field studies have reported successful application of the FBWFs in single and multi-layer tight formations. Recently, the ability of FBWFs in controlling well kick and potential blowout, modification of the strength and other mechanical properties of coal seams, enlargement of the safe operating zone of coal seam wells, prevention of water invasion, the dispersion of coal fines in coalbed methane reservoirs (CBMs), enhanced oil recovery operations, effective control of wellbore instability, and its eco-friendliness have been extensively studied (He et al., 2021; Wang et al., 2016; Wei et al., 2020; Zhang et al., 2019; Zheng et al., 2018). Despite fulfilling the engineering and reservoir damage control requirements in the field, to date, no study has addressed the degree of fuzzy-ball-induced damage and its reservoir damage mechanism in single and multi-layer reservoirs. Furthermore, it is important to examine the damage-control mechanisms of the fuzzy-ball fluids at a microscopic scale and establish an optimal field application technique that would guide the future implementation of FBWFs in single and multi-layer reservoirs. Of course, there are many methods for studying reservoir damage (Lin et al., 2017). In this study, sets of experiments (such as microscopic testing, core flooding, and SEM/EDS test) were conducted to evaluate the mechanisms and degree of fuzzy-ball-induced damage to single and double-layer tight reservoirs via microscopic analysis, permeability, and flow rate indexes. Samples from the Linxing area in the eastern part of Ordos Basin were randomly selected in addition to the two carbonate samples from the middle Ordovician zones of the Shunbei Oilfield utilized in the SEM/EDS experiment. An FBWF was formulated following a specified design range. This study made the following specific scientific achievements: (1) Pioneers the evaluation of the degree of fuzzy-ball-induced damage in single and multi-layer reservoirs. (2) Further validates the newly established flow rate formation damage evaluation index. (3) Establishes the formation damage mechanisms and the damage control techniques of FBWFs. In general, the research findings will provide a reliable basis for lab-scale evaluation of reservoir damage induced by other fluid types, guide field experts during the future application of FBWFs, and serve as a theoretical basis for optimal design and application of low-damaging fluids in petroleum reservoirs.

2. Experimental section

2.1. Fuzzy-ball working fluid design and formulation experiment

During this experiments, fuzzy-ball drilling and completion fluids were formulated by adding, 0.2 wt% sodium hydroxide (SOH), 2 wt% fuzzy-ball coating agent (FBCA), and 0.8 wt% fuzzy-ball floss agent (FBFA) into a blending container of warring blender containing 200 mL of deionized water. Then it was blended at a shearing rate of 8000 r/min for 50 min. To ensure that the added chemical reagents were evenly dispersed, 0.3 wt% of fuzzy-ball core agent (FBKA) and 0.6 wt% of fuzzy-ball membrane agent (FBMA) were slowly added and stirred at the same shearing rate for another 50 min. During the formation damage evaluation test, the rheological properties such as density, plastic viscosity, and apparent viscosity of the prepared fluid were maintained at 0.81 g/cm^3, 17 mPa s, and 36.3 mPa s, respectively at a stable pH of 9.0 ± 0.1. The ionic strength of the fluid was stabilized at 0.1 M to meet the application design requirements of coal seams (Awan et al., 2020). The design components namely, composition, molecular formula, purpose, and range of concentrations of the chemical reagents of the fuzzy-ball drilling and completion fluid are shown in Table 1.

2.2. Microscope experiment

The main objective of this experiment is to observe the molecular structure of fuzzy-ball fluids. Samples of the fuzzy-ball fluid were placed under an optical microscope. The resultant micrographs were observed and captured under a 1500 times microscope. The characteristics of FBWFs are investigated through their microscopic structure.

Table 1
Design components of fuzzy-ball drilling and completion fluids.

Reagents	Chemical name	Chemical formula	Purpose	Conc., wt%
FBCA	HES	$C_{22}H_{44}O_{17}$	Strength enhancement	2.0–2.5
FBFA	PAC	$[C_6H_7O_2(OH)_2OCH_2COONa]_n$	Floss generation	0.8–1.0
FBKA	SDS	$C_{12}H_{25}SO_4Na$	Improve plugging ability	0.2–0.4
FBMA	SDBS	$C_{18}H_{29}NaO_3S$	Enhance the dispersion of fines	0.4–0.8
NaOH	SOH	NaOH	Control the pH value	0.2–1.0

2.3. Formation damage evaluation experiments

In this experiment, we mainly evaluate the degree of fuzzy-ball damage in single-and multi-layered commingled reservoirs. In this regard, a series of single and double-layer core flooding experiments are carried out. The degree of fuzzy-ball damage is estimated using permeability and flow rate indexes.

2.3.1. Materials

The experimental materials include formation water, nitrogen gas, core samples, and fuzzy-ball fluid. Formation water was used to determine the initial water saturation of core samples. Formation water types and salinity were consistent with previous studies (Liu et al., 2022). The composition and preparation process of the fuzzy-ball fluid are discussed in section 2.2. Nine combinations of sandstone and coal samples from well LS of the Linxing area in the eastern part of Ordos Basin, China, were randomly selected from the Shanxi, Taiyuan, and Benxi formations to perform the formation damage evaluation experiment (Appendix B). According to the guidelines of China's industry best practices for core analysis (SY/T 5336–2006), the selected core samples (Table A1) were prepared. Based on China's industry standards for reservoir sensitivity experiments (SY/T 5358–2010), the selected core plugs were cut into a diameter of 25 mm with a length-to-diameter ratio of 1.5. Three core samples were used for the single-layer experiment and three groups of different core combinations were assigned for the double-layer experiment (Table A2).

2.3.2. Experimental setup

The experimental apparatus of the single-layer experiment consists of a data collection unit, pressure gauge, confining pressure pump, core holder, transfer vessel, and injection pressure pump (Fig. 1).

As shown in Fig. 2, the experimental setup consists of six units: (a) gas storage and supply unit, which includes an air compressor, nitrogen tank, and fluid cylinder; (b) measuring and pressure control unit, which comprises of a pressure gauge, valves, and sensors; (c) core sample holding devices, comprising of 25 mm diameter core holders, heating jackets, and confining pressure pumps; (d) flowmeter unit, that consist of flowmeters at different sections; (e) wellbore simulator; and (f) data collection unit.

2.3.3. Experimental procedure

2.3.3.1. Single-layer formation damage evaluation experiment. The single-layer formation damage experiment involved three stages as highlighted below (Zheng et al., 2021):

Stage I (saturate the core with formulated brine): Insert a dry core into the core holder and turn the three-way valve to apply a confining pressure of 5 MPa (Fig. 1). Then inject the formation brine at specified flow rate to saturate the core. Stop the saturation process for 12 h to prevent distortion of the fracture geometry due to induced stress. Then re-inject the formation brine at the same flow rate as the first injection scheme. Based on the pressure difference across the injection stages, estimate the permeability and instantaneous flow rate.

Stage II (damage core plugs with the FBWFs): Open the two-way valve to inject FBWF into the core. Given that FBWFs are viscous, it is precautionary to inject the fluids at a constant pressure of 3.5 MPa for 2 h. To effectively simulate the reservoir damage of FBWFs under laboratory conditions, the FBWF is sequentially injected into core samples following the requirements of China's industry standard (SY/T 6540–2002). The core flooding process is performed under constant pressure condition and a flooding temperature of 20 °C.

Stage III (estimate the fuzzy-ball induced damage to the core samples): Re-inject the formation brine into the cores following the

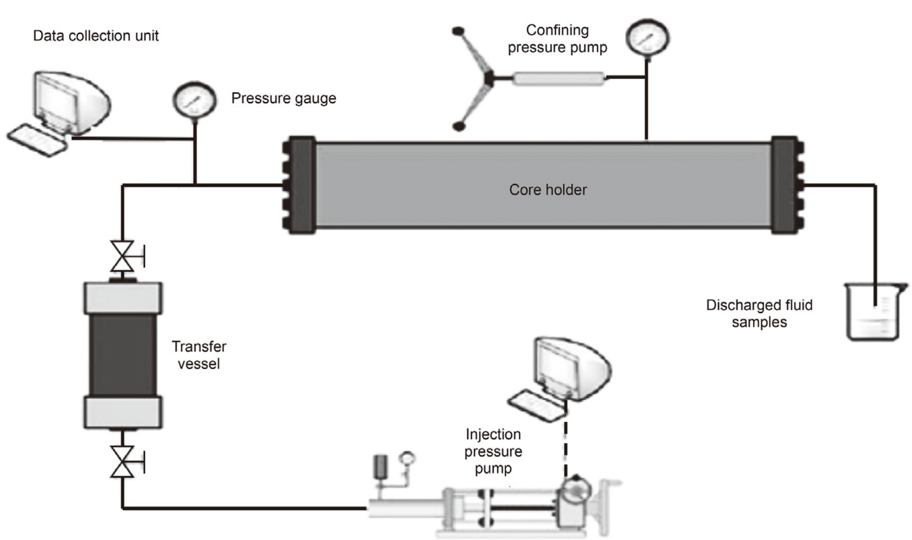

Fig. 1. Schematic diagram of the single-layer formation damage evaluation experiment.

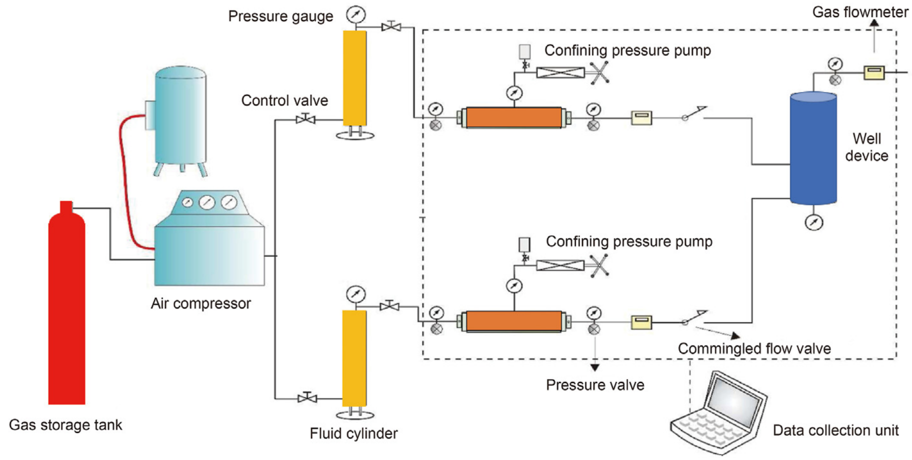

Fig. 2. Schematic of double-layer formation damage experiment.

same procedure in Stage I. Observe the pressure, and estimate the permeability and instantaneous flow rate after steady state is attained. The instantaneous flow rate is measured every 0.5 min before and after fuzzy-ball damage at four consecutive intervals.

Based on the pressure gradient of the overburden layer of Linxing Formation estimated as 0.023 MPa/m, thus the equivalent confining pressure of the tight sandstone reservoir is about 30 MPa, and that of the coal seam is about 34 MPa (Liu et al., 2022). In this regard, it is expected to adjust the increasing rate of the inlet pressure, and gradually increase the overburden pressure. The pressure is adjusted between 1.5 and 2.0 MPa above the inlet pressure until it reached 30 and 34 MPa for the sandstone and coal samples respectively. A summary of the experimental conditions for different core samples during the single-layer experiments is shown in Table 2.

2.3.3.2. Double-layer formation damage evaluation experiment. Since tight reservoirs lacks adequate thickness to economically produce, petroleum reservoirs are mainly developed by multi-layer commingled production systems from a single vertical well (Fig. A2). To effectively simulate formation damage in multi-layer system, the double-layer simulation experiment offers a comparative advantage over the single-layer experiments. More so, in the double-layer simulation experiments, the effect of interlayer interference and other variation in reservoir properties are considered. The double-layer simulation experiment follows a similar procedure to the single-layer experiment, except for two differences. Firstly, the two core samples are separately loaded into the upper and middle core holders, respectively, and ensure the joints are tightly connected to avoid leakage (Fig. A2). Secondly, based on the variation of *in-situ* stress per depth, the overburden pressure of both layers will be different. Therefore, a different confining pressure is maintained for both core samples throughout the experiment. The core flooding process is performed under constant pressure condition and a flooding temperature of 20 °C. A summary of the experimental conditions for different core sample combination during the double-layer commingled reservoir experiments is presented in Table 3.

2.3.4. Data analytical approach

According to the principle of the permeability evaluation index, the gas permeability (K_g) is calculated by Darcy's equation using

$$K_g = \frac{2P_a \times Q \times \mu \times L}{\left(P_1^2 - P_2^2\right)A} \times 100 \quad (1)$$

where P_a is the atmospheric pressure (MPa); Q is the stable flow-rate (cm^3/s); μ is fluid viscosity at the test condition (mPa·s); L is length of core sample (cm); and P_1 *and* P_2 is the inlet and outlet pressure respectively (MPa).

For cores damaged by working fluids, the permeability damage rate (D_p) becomes

$$D_p = \frac{\left|K_f - K_i\right|}{K_i} \times 100\% \quad (2)$$

$K_i, K_f,$ represents permeability before and after damage by working fluids respectively ($10^{-3}\mu m^2$).

For the flow rate evaluation index, the estimated flow damage rate (D_F) is given by

Table 2
Experimental conditions of single-layer experiments.

Sample	Lithology	Damage state	Inlet pressure, MPa	Outlet pressure, MPa	Time, min
LS-2	S	Before	14.62	0.16	135.5
		After	14.66	0.14	
LS-4	S	Before	14.54	0.16	105
		After	14.53	0.15	
LC-1	C	Before	16.47	0.16	109
		After	16.45	0.13	
LC-5	C	Before	16.36	0.16	120.5
		After	16.39	0.14	

Table 3
Experimental conditions of double-layer commingled reservoir experiments.

Sample	Damage state	Core	Inlet pressure, MPa	Outlet pressure, MPa	Time, min
LS-6 + LC-2	Before	S	12.54	0.14	86
		C	14.55	0.14	
	After	S	12.53	0.12	
		C	14.57	0.12	
LC-3 + LS-8	Before	C	14.58	0.14	87
		S	12.49	0.14	
	After	C	14.57	0.12	
		S	12.52	0.12	
LS-10 + LC-4	Before	S	12.53	0.14	84
		C	14.55	0.14	
	After	S	12.52	0.12	
		C	14.48	0.12	

Note: The observed slight difference in injection pressure of sandstone and coal samples accounts for the variations in confining/overburden pressure of both cores under *in situ* conditions (Liu et al., 2022).

$$D_F = \frac{Q_{os} - Q_{ds}}{Q_{os}} \times 100\% \quad (3)$$

Q_{os}, Q_{ds}, represents instantaneous flow rates before and after damage by working fluids respectively (cm^3/s).

From Darcy's equation (Eq. (1)), the flow rate and permeability are linearly related provided that other parameters in the equation are known (constant). Therefore, the relationship between flow rate and permeability before and after working fluid damage can be written as

$$D_F = \alpha D_p + \beta \quad (4)$$

From Eq. (4), α and β can be calculated using

$$\alpha = \frac{P_1'^2 - P_2'^2}{P_1^2 - P_2^2} \quad (5)$$

$$\beta = \frac{\left(P_1^2 - P_2^2\right) - \left(P_1'^2 - P_2'^2\right)}{P_1^2 - P_2^2} \quad (6)$$

where P_1 is the core inlet pressure before damage by working fluid (MPa); P_2 is the core outlet pressure before damage by working fluid (MPa); P_1' is the core inlet pressure after damage by working fluid (MPa); P_2' is the core outlet pressure after damage by working fluid (MPa).

The corresponding permeability recovery rate for each core sample is

$$\text{Permeability recovery rate } (\%) = \left(\frac{K_f}{K_i}\right) \times 100 \quad (7)$$

2.3.5. SEM/EDS experiments

The SEM/EDS testing was carried out to observe the chemical and morphological changes, and nanoscale structural changes due to potential fuzzy-ball-induced damage on tight reservoirs. Two carbonate samples from the middle Ordovician zones of the Shunbei Oilfield, China were used for the SEM/EDS experiment. The cores were chosen from oil and gas fields in which the fuzzy-ball fluids have been previously applied. The specifications of the selected cores are shown in Table A1.

Several studies have demonstrated the utilization of this technique in providing detailed magnification information on the seepage channel configuration, pore topological structure, pore morphology, and porosity distribution of core samples of different lithologies (Chen et al., 2017; Halim et al., 2021; Scimeca et al., 2018; Yang et al., 2021). SEMs are devices that produce a highly magnified image of a sample by scanning it with a focused beam of electrons. During an SEM experiment, several electrons are thermionically transmitted from an electron gun containing a tungsten filament cathode that is placed on top of the microscope. These transmitted electrons are focused along a vertical plane toward the sample. When the electrons encounter the sample, they interact with atoms in the sample and emit some secondary electrons by inelastic scattering. These electrons are characterized by low energy (less than 50 eV) and a low travel distance from the surface of the sample (de Assumpcão Pereira-da-Silva and Ferri, 2017). Because SEM employs excited electrons for imaging, studies have shown that the electron microscope must act in a high vacuum environment such that the electrons are not absorbed by the atmospheric molecules as they move to the sample and detector (Sokolov et al., 2016). In this regard, it is expected to ensure a high vacuum condition during the SEM experiment.

The core samples namely, SC-0, LS-12, and LC-6 (Table A1) were used during the SEM testing. First, the dry cores were inserted into the sample chamber through the sample holder. Then the focus, magnification, brightness, and contrast were gradually adjusted until the desired image quality was obtained. Finally, the sample is removed and obtained results were recorded via the backscattered electron detector and secondary electron detector installed in the computer unit. The experiment was performed for the dry cores and was repeated after the samples were treated with the FBWFs for 48 h.

The EDS is a non-destructive method that measures the characteristic X-rays emitted from materials exposed to high-energy electrons during the SEM test (Sokolov et al., 2016). It mainly involves the interaction of an electron with an atom causing the inner shell electron from the atom to be ejected. The void space created will be filled by an electron from a higher energy level. During this process, an X-ray will be emitted and energy is conserved. Since the generated energy is different for each chemical element, the element can be identified by the emitted X-ray (Fig. A3). Similar equipment, procedure, and core plugs as in the SEM experiment were used for the EDS experiments. However, for the EDS test, data were collected using an EDAX Octane Elect Plus EDS detector and the TEAM software package.

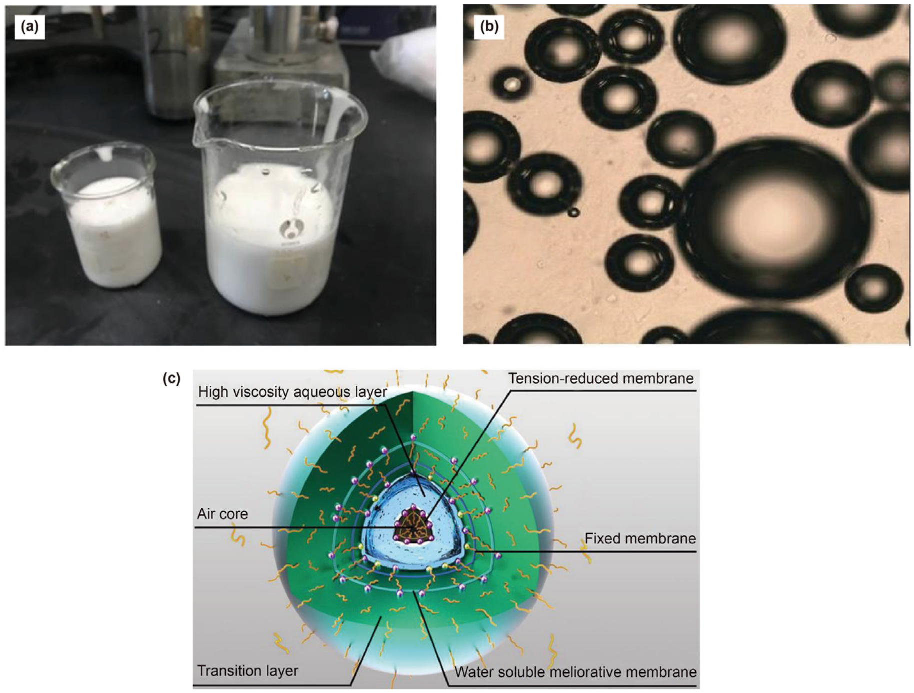

Fig. 3. Components of the FBWFs (**a**) samples of FBWFs; (**b**) micrograph of fuzzy-balls under 1500 times microscope; (**c**) schematic of the vesicle structure of a fuzzy-ball in a liquid phase (Wei et al., 2020).

3. Results and discussion

3.1. Analysis of microscopic properties of FBWFs

Based on the results of the microscopic observation and testing, the micrograph of an FBWF is shown in Fig. 3.

The microstructure and flow behavior of the fuzzy-ball fluid vary in static and dynamic conditions during application. In a static state, the inner segment contains an air-core while the outer surface is in the form of fuzz of high gel strength. In a dynamic state, the well-distributed fuzz in the liquid phase is composed of different sizes that are flexible enough to improve the overall flowability of the fluid (Fig. 3(b)). When dissolved in dispersing agents, an equilibrium phase comprising gas and liquid is formed. The formulated system majorly comprises one air core, two layers (transition and large viscous solution layers), and three outer layers (tension-reduced, fixed, and water-soluble membranes). The air core is known as the vesicle (Fig. 3(c)). The vesicles are low-density phases composed of the anionic surfactants (SDBS and SDS) specified in Table 3. Further, they are characterized by large deformability and ductility which varies from 15 to 150 μm (Wei et al., 2020). They are stable in water-based fluids and compatible with formation water, polymers, and other displacement systems (He et al., 2021). The fuzzy-ball drilling fluids are characterized by high viscoelasticity, and shear-thinning ability, and are very stable in high-salinity formation brines (Wei et al., 2018).

3.2. Analysis of fuzzy-ball-induced damage in single and double-layer reservoirs

3.2.1. Analysis of fuzzy-ball-induced damage in single-layer reservoirs

Based on the single-layer experimental process described in section 2.3.3.1, the recorded experimental data before and after fuzzy-ball-induced damage on core samples from various stratum are presented in Table 4.

Substituting the permeability and flow rate data in Table 4 into Eqs. (2) and (3) respectively, the permeability and flow damage rate are computed for a single-layer reservoir, the results are shown in Fig. 4.

Combining the standard classification of formation damage (Table A3) and the results of Fig. 4, it is evident that for coal seams, the FBWFs induced weak damage on the core samples. This is because, despite the unconsolidated nature of coal samples, the fuzzy-ball fluid provided a high seepage blocking ability which improves the strength of the core, and the dispersion of coal fines

Table 4
Experimental data of fuzzy-ball-induced damage in single-layer reservoirs.

Sample	Lithology	Damage state	Permeability, 10^{-3} μm^2	Instantaneous flow rate, cm^3 s^{-1}
LS-2	S	Before	0.008683	4.928148
		After	0.005779	3.296530
LS-4	S	Before	0.004225	2.350000
		After	0.002820	1.566667
LC-1	C	Before	0.002133	1.628751
		After	0.001980	1.499437
LC-5	C	Before	0.001665	1.224508
		After	0.001540	1.138366

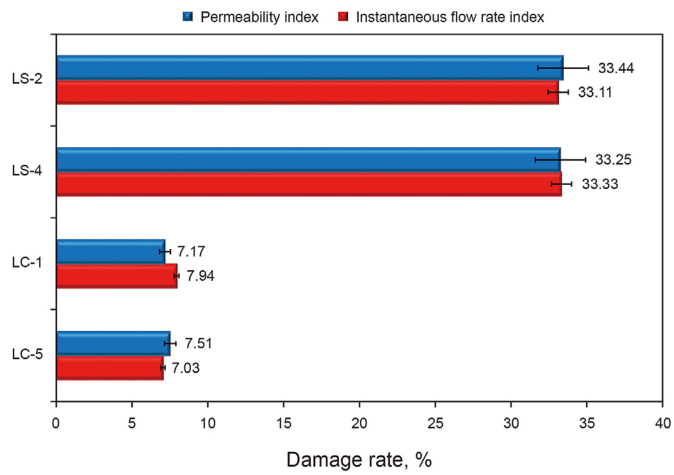

Fig. 4. The damage rate of fuzzy-ball fluid for instantaneous flow rate and permeability indicators in single-layer development.

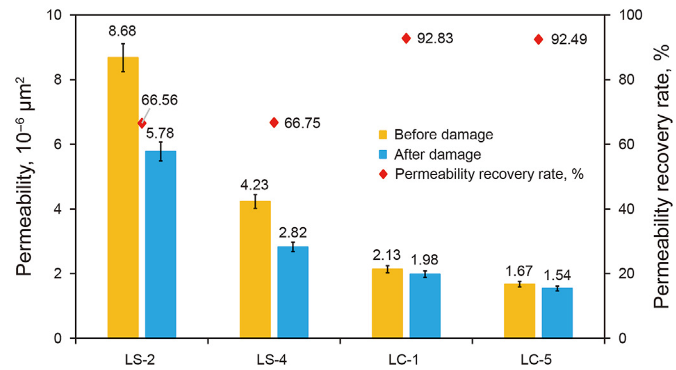

Fig. 5. The permeability recovery rate of core samples after fuzzy-ball-induced damage.

by the SDBS (Awan et al., 2020; Ur Rahman Awan et al., 2019). More so, the fuzzy ball fluid-induced medium to weak damage to the sandstone samples. Given that minerals in tight sandstone reservoirs tend to be strongly water-wet (Chima et al., 2018; Byrne et al., 2000), FBWFs are easily imbibed into formations by strong capillary pressure, thereby blocking the effective flow path of oil/gas from the reservoir to the wellbore.

The results of Fig. 4 indicate that the estimates from the instantaneous flow rate index of four core samples are almost similar to the corresponding permeability indicator. The damage classification offered by both indicators was consistent with an absolute error between 0.08% and 0.77%. This trend conforms with the findings from previous scholars (Liu et al., 2022). It further validates that the flow rate method could be utilized as a substitute index to the conventional permeability method, for determining the degree of working fluid damage in single-layer reservoirs. Additionally, it confirms that there is a linear relationship between instantaneous flow rate and permeability indicators in single-layer reservoirs. The difference between the instantaneous flow rate and permeability indicators in single-layer is within 1%, hence the use of the flow rate index in the evaluation of reservoir damage is more intuitive. Therefore, based on experimental analysis, for a single-layer reservoir system, the degree of formation damage caused by the fuzzy-ball fluids is minimal, which conforms to the reservoir protection requirements for the application of working fluids in petroleum reservoirs. Additionally, the flow rate method can potentially be used as a substitute for the permeability method during the laboratory estimation of working fluid damage in single-layer formations.

By depth and stratum, according to the results of Fig. 4 and core specification in Table A1, the damage rate of the fuzzy-ball fluids in the upper zones (LS-2 and LS-4) was higher than in the lower zones (LC-1 and LC-5). Furthermore, the fuzzy-ball fluid resulted in higher damage to the sandstone formation at the upper Taiyuan formation than the sandstones at the upper Shihezi Formation. The permeability damage rate of the lower Shanxi Formation was higher than the lower Taiyuan Formation. The largest formation damage existed in the upper Taiyuan Formation at 33.44%. Although the difference in the induced damage was not significant, however, it is an important detail that could guide future applications.

As Fig. 5 shows, the presence of FBWFs appears to slow down the chemical reaction between the fluid and rock, reducing the rate of permeability improvement. After fuzzy ball damage, the permeability recovery rate of the coals was higher than the sandstones. A possible explanation is that after the application of fuzzy-ball fluids, the fluid degrades naturally, and its residue will lead to low damage to the reservoir. More so, the presence of anionic surfactants such as SDS and SDBS in FBWFs (Table 1) enhance their plugging strength and the dispersion of generated coal fines that could potentially lead to formation damage hence, increasing the permeability recovery rate in coals (He et al., 2021; Awan et al., 2020). Based on the high permeability recovery rate and low matrix damage of the fluid, the overall well performance is enhanced, and the intended field operation will be executed successfully.

3.2.2. Analysis of fuzzy-ball-induced damage in double-layer commingled reservoirs

Based on the double-layer experimental process described in section 2.3.3.2, the recorded experimental data before and after fuzzy-ball-induced damage on core samples from various stratum are presented in Table 5.

As can be seen from Tables 5 and in the case of the double-layer systems, the combined permeability damage rate cannot be quantitatively measured. This is attributed to the difference in core parameters such as the inlet and outlet pressure, length, and diameter (Liu et al., 2022). In addition, the significant difference in the *in-situ* stresses of each layer will limit the experimental process.

Comparing the results of Table 5 with previous studies, the experimental data of working fluid damage in double-layer commingled systems agrees with the outcomes of similar research (Liu et al., 2022). This further justify the applicability of the flow rate indicator in evaluating formation damage in multi-layer reservoirs. Therefore, the results of Table 5 validate the correctness of the fundamental and experimental parameters setup and verify that the flow rate method can precisely evaluate fuzzy-ball induced damage in multi-layer reservoirs. Substituting the flow rate data in Table 3 into Eq. (3), the flow rate damage rate is computed for double-layer commingled reservoirs, the results are shown in Fig. 6.

Similar to the case of single-layer reservoirs, it can be seen from Fig. 6 that the fuzzy-ball fluid-induced weak damage on the core samples with a maximum damage rate of about 8.56%. This result agrees with the outcomes of the application of fuzzy-ball fluids in field-scale. Combining the results of the single and double-layer working fluid damage experiments, the fuzzy-ball fluid-induced lower damage in double-layer reservoirs than the single-layer reservoirs. This can be attributed to the fact that in single-layer reservoirs, the fundamental mechanisms of formation damage are generally classified into mechanical, chemical, biological and thermal mechanisms (Lin et al., 2020; He et al., 2021; Okere et al., 2020). However, for double-layer commingled reservoirs, in addition to

Table 5
Experimental data of fuzzy-ball-induced damage in double-layer reservoirs.

Sample	Damage state	Core	IP, 10^{-3} μm^2	OP, 10^{-3} μm^2	IIF, cm^3 s^{-1}	OIF, cm^3 s^{-1}
LS-6 + LC-2	Before	S	0.00493	N/M	2.460000	3.430000
		C	0.00189		1.250000	
	After	S	0.00289	N/M	2.227778	3.160000
		C	0.000124		0.972222	
LC-3 + LS-8	Before	C	0.006317	N/M	2.787566	3.116667
		S	0.002586		1.193333	
	After	C	0.004101	N/M	2.574444	2.850000
		S	0.000301		0.250000	
LS-10 + LC-4	Before	S	0.003968	N/M	2.805558	4.027578
		C	0.002317		1.633333	
	After	S	0.002475	N/M	2.450000	3.706177
		C	0.000354		1.220315	

Note: IP: Individual permeability; OP: Overall permeability; IIF: Individual instantaneous flow rate; OIF: Overall instantaneous flow rate; N/M: Not measurable.

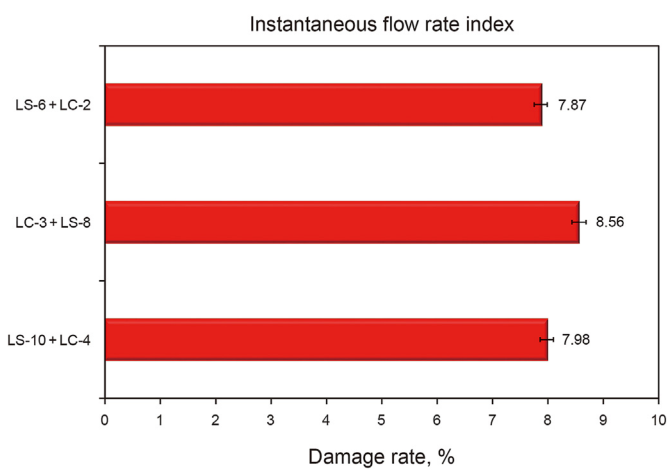

Fig. 6. Estimated damage rate of FBWFS in double-layer reservoirs via flow rate index.

the fundamental causes of reservoir damage, interlayer interference significantly influences the damage rate (Ding et al., 2019; Tao et al., 2022). Given that the average damage degree of sandstone and coal are less than 10%, the experimental results meet the reservoir protection requirements of the working fluid.

3.3. Analysis of reservoir-fuzzy-ball fluid interaction-related formation damage

The microscopic observation of the cores revealed that the pore system was predominantly a secondary pore with few numbers of primary pores. The results of the dry SEM analyses (Fig. 7) showed that the cores comprise evenly distributed fine grains and laminations. The major framework grains in the coal samples were pyrites and clay with minimum quartz (Fig. 7(a)). The quartz grains are the main cementing minerals while the clay minerals are mainly lamellar and platelike. High content of quartz minerals is nonuniformly distributed in the sandstone (Table A4). Also, some fragments of feldspar and clay particles could be seen in the micrograph. The clay is mainly composed of chlorite, smectite, kaolinite and illite (Table A5). Cell-filling clay minerals adhered to the surface and traces of dispersed clay minerals were extensively found in raw samples, distributed as fine grains. In the carbonate sample (Fig. 7(c)), calcite minerals can be predominately distributed with few traces of dolomites. The dolomites were observed along the fractured zones. Overall, the dry samples are characterized by micropores with natural and induced fractures.

The SEM photomicrograph shows no significant microscopic variations in the cores after treatment. Traces of the solids from the FBWFs were observed on the pores of all three samples with no evidence of fines migration. Studies have shown that the main parameter that determines the degree of permeability alteration reaction is the geometric disposition of the clay minerals in the

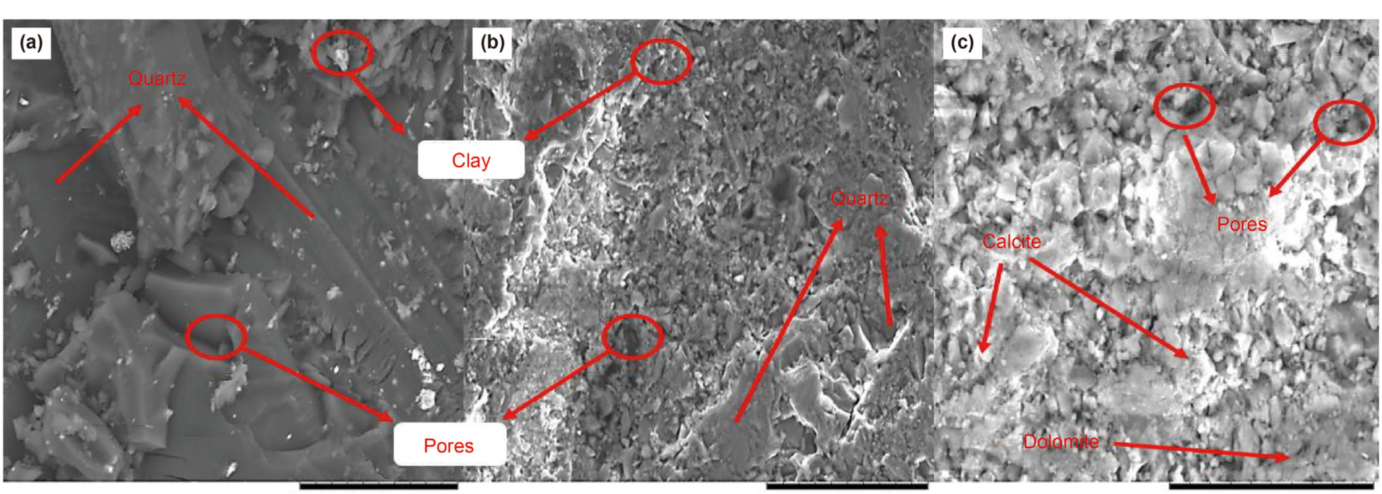

Fig. 7. SEM results of untreated core samples (**a**) coal (**b**) sandstone (**c**) carbonate.

Petroleum Science 20 (2023) 3598–3609

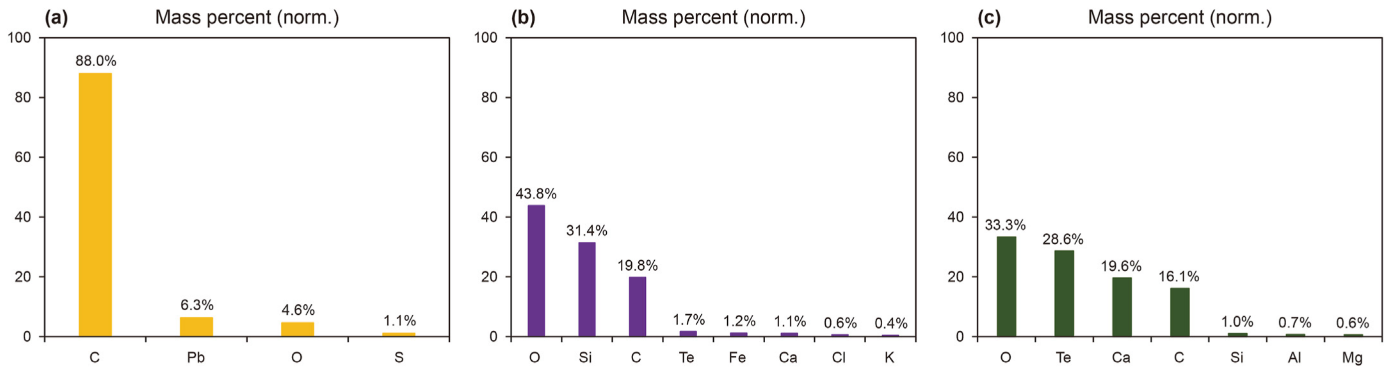

Fig. 8. EDS results of untreated core samples (**a**) coal (**b**) sandstone (**c**) carbonate.

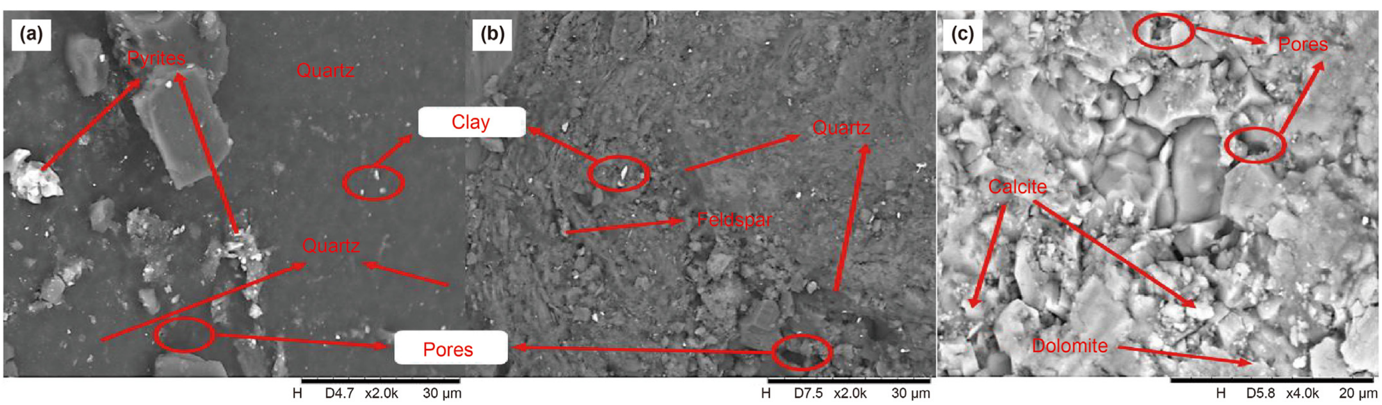

Fig. 9. SEM results of treated core samples (**a**) coal (**b**) sandstone (**c**) carbonate.

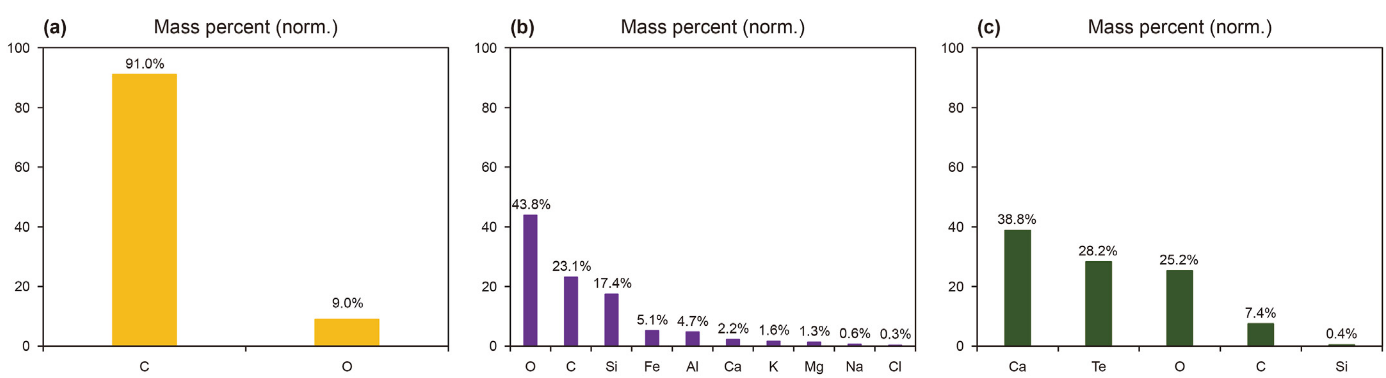

Fig. 10. EDS results of treated core samples (**a**) coal (**b**) sandstone (**c**) carbonate.

micropore system (Bourg and Ajo-Franklin, 2017; Chagneau et al., 2015; Halim et al., 2021). Hence as Fig. 7(a) shows, before damage the amount of clay-bearing mineral in the pore system is relatively small. After damage (Fig. 9(a)), there was no significant alteration in the mineral composition of the samples. The clays were tightly bonded to the rock surfaces due to the strong bonding ability of FBWFs. Therefore, the possibility of the occurrence of formation damage due to clay swelling or the generation of fine particles is minimum.

The EDS results in Figs. 8 and 10 show dissolution and precipitation of some chemical elements after treatments. The dissolution of Lead (Pb) and Sulfur (S) occurred in the coal seam, while Tellurium (Te) in sandstone, Aluminum (Al), and Magnesium (Mg) in carbonate. However, the precipitation of Al, Mg, and Sodium (Na) occurred in sandstone with no precipitation in coal and carbonate. These precipitates could lead to fine migration and solid invasion thereby reducing effective formation permeability. Several scholars have provided convincing evidence that revealed that these precipitations often occur in sandstone formations (Chima et al., 2018; Potysz and Bartz, 2022; Shafiq and Mahmud, 2017). Further, the properties of sandstone formations enable the aggregation of fines which will precipitate sands and result in the clogging of the pore throats and permeability impairment (Wetzel et al., 2020). The EDS analysis has shown that the FBWF only slightly alters the microscopic components of a reservoir. The precipitation impact of the FBWFs on core plugs is minimal, suggesting that the risk of reservoir damage due to fine migration is minimal in sandstone formation and does not exist in coal and carbonate formations.

Dolomite and calcite minerals dissociate in working fluids to generate new precipitates. In addition, these minerals are less cemented and could easily be detached by fluid flush (Tan et al., 2021). However, the result of the EDS experiment shows that the FBWFs did not induce precipitate in the calcite-rich carbonate core sample. One explanation for this is that FBWFs are not fluorine ion-bearing fluids that often form new precipitates in a solution (Tan et al., 2021). The main rock-forming minerals like quartz and feldspar are very sensitive to alkaline solutions thereby dissolving to form precipitates that will induce mechanical damage to the reservoir (Yuan and Wood, 2018). Also, carbonate cores contain salt minerals such as magnesium and calcium, which when dissolved in low-salinity fluids, weaken the rock matrix and result in fine migration (Huang et al., 2015, 2018; Katende and Sagala, 2019). However, the plugging of the flow zones by FBWFs enables it to modify the mechanical property of the rock and increase the rock strength (Zheng et al., 2018).

3.4. Recommendations for the damage-mitigation approach of fuzzy-ball fluids

The FBWFs contains several chemical compounds within specified design requirements (Table 1). These chemicals could potentially lead to adverse rock-fluid or fluid-fluid interactions that can negatively impact the reservoir (Liang et al., 2017; Wuyep et al., 2020; Zheng et al., 2017). In this section, recommendations on the formation of damage-prevention mechanisms and design specifications are presented.

Formation damage mainly emanates from both the physical and chemical effects of the particles and the fluid that invades the reservoir (Lin et al., 2020; Okere et al., 2020). Therefore, minimizing the invasion of water-based fluids is critical for damage control. An effective method for controlling formation damage caused by water-based fluids is through a rapid and efficient plugging and the adjustment of the rock-fluid compatibility (Al-Ajmi et al., 2017; Guo et al., 2020). If these two parameters are adequately controlled, the reservoir protection ability of fuzzy-ball working fluid could be greatly improved, and the degree of formation damage will be significantly minimized.

Regarding the plugging ability, several fields, and laboratory studies have shown that FBWFs provide excellent plugging strength which further improves the mechanical properties of the reservoir rock (He et al., 2021; Zheng et al., 2016; Zheng et al., 2018). However, the rate of plugging varies with the width of the seepage channels (Yang et al., 2013; Zhu et al., 2018). When the width of the seepage channel is smaller than the effective diameter of the vesicles, the rate of plugging is relatively faster, however, if the width of the seepage channel is equal to the size of the vesicles, the rate of plugging becomes moderate. The least rate of plugging is experienced when the width of the fracture is larger than the vesicles (Fig. 11). Therefore, the most rapid and effective plugging offered by the FBWFs occurs when the width of the seepage channels is smaller than the effective diameter of the vesicles. This is because, the reservoir will be quickly and tightly sealed, and the permeability of the reservoir will be efficiently restored thereby minimizing potential permeability damage.

Another possible explanation of the plugging ability of the FBWF implies that during injection, the vesicles of the fuzzy ball aggregate and plug the seepage zones (Fig. 11). Furthermore, the accumulated vesicles form a floss structure that facilitates the accumulation of different flosses around the seepage channels. Hence, the intermolecular bonds within the vesicles are significantly increased thereby improving its plugging strength. FBWFs are characterized as hydrophilic fluids, hence, they exhibit a high affinity for formation water which is beneficial to the long-term prevention of water encroachment.

The temporary plugging function offered by the FBWF is mainly a plugged zone formed within the pore throats or fractures and the creation of a sealing structure around the seepage channels that protects the reservoir. The major difference between these plugging systems is the plugging rate and depth of invading filtrate. Therefore, the degree of reservoir damage and efficiency can also provide a reference for effective protection. Compared with other water-based fluids, the chemical components of the FBWFs are more compatible with reservoir fluids. The floss control agent and other four reservoir-friendly additives play a vital role in minimizing fluid loss. These chemical compounds constitute the main components of the damage-control technology of FBWFs, and they should meet the compatibility between materials as well as the high plugging strength requirements.

The damage-control mechanism of FBWF is limited by the uncontrolled volume of the base fluid. This could result in rock-fluid compatibility issues, precipitations, clay swelling, and deflocculation. More so, the high pH value of the formulated fluid could lead to alkaline sensitivity damage. In this regard, it is recommended to control the composition of the base fluid within the design limit, and distilled water should be utilized. In addition, the ionic strength of the fuzzy ball fluid should be designed to meet the specific requirements of the intended reservoir. Finally, weighting agents and pH controlling agents should be selected according to actual geological conditions, considering cost and efficiency.

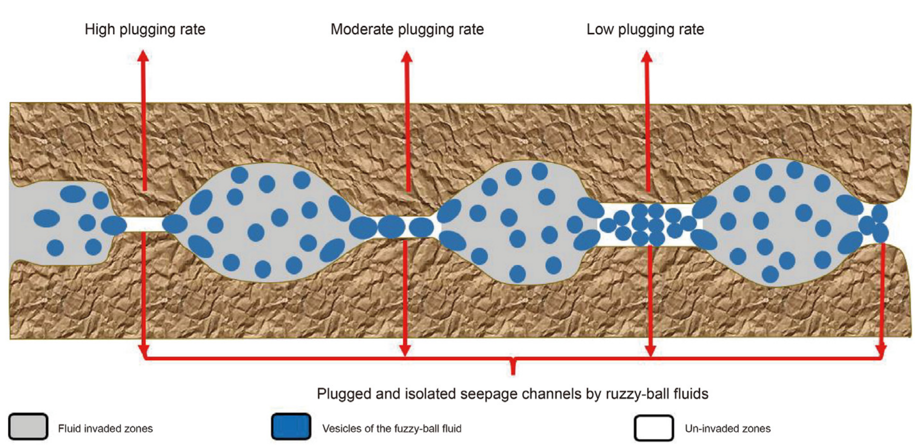

Fig. 11. Fluid invasion-control mechanisms by FBWFs.

4. Conclusions

Through carefully designed and executed experiments, this study confirms that the FBWFs induce low damage in single and double-layer reservoirs by two evaluation indexes, namely the permeability and the flow rate index. Microscopic experiments were performed to visualize the microstructure of cores before and after fuzzy-ball-induced damage. The following conclusions were obtained.

1. In the single-layer reservoir system, fuzzy-ball fluids induced weak damage on coals and medium-to-weak damage to sandstones. The permeability recovery rate after damage by fuzzy-ball fluids was higher in coals than in sandstones. Based on the depth and stratum, the damage rate in the upper zones was higher than in the lower zones with the highest damage degree at 33.44%.
2. In the double-layer commingled reservoir system, fuzzy-ball fluids induced weak damage and the degree of fuzzy-ball damage in double-layer commingled formations were lower than the single-layer reservoirs, indicating that FBWFs are low-damaging multi-layer commingled reservoir-friendly fluids.
3. After damaged by the FBWF, no significant changes occurred in the microstructure of the cores as traces of vesicles were observed on the pores with no evidence of fines migration. The dissolution of Pb and S occurred in the coal seam, while Te in sandstone, and Al, Mg in carbonate. However, the precipitation of Al, Mg, and Na occurred in sandstone with no precipitates found in coal and carbonate.
4. The temporal plugging and dispersion characteristics of the fuzzy-ball fluids enable the generation of reservoir protection layers that minimizes formation damage due to solid particle and fluid invasion. However, the plugging rate is critical to its performance and future research could explore this direction.

Declaration of competing interest

We wish to confirm that there are no known conflicts of interest associated with this publication and there has been no significant financial support for this work that could have influenced its outcome.

Acknowledgments

The authors wish to thank the Ministry of Science and Technology of the People's Republic of China (2016ZX05066). Chinedu J. Okere appreciate the Distinguished Graduate Student Fellowship from Texas Tech University, United States of America. The author greatly appreciates the equipment support provided by the Fragmented Reservoir Research Center of Beijing LihuiLab Energy Technology Co., Ltd., a CNAS internationally recognized laboratory. Thank you to the experts from the Sealaplugology Professional Committee for providing on-site data assistance.

Appendix A. Supplementary data

Supplementary data to this article can be found online at https://doi.org/10.1016/j.petsci.2023.05.017.

Nomenclature

FBWF	Fuzzy-ball working fluid
CBM	Coalbed methane
SEM	Scanning electron microscope
EDS	Energy-dispersive spectroscopy
CT	Computed tomography
IMEXTM	Ion mobility expansion
CMG	Computer Modelling Group Ltd.
NMR	Nuclear magnetic resonance
PTT	Pressure transmission test
SDBS	Sodium dodecyl benzene sulfonate
SDS	Sodium dodecyl sulfate
HES	Hydroxyethyl starch
PAM	Polyacrylamide
SOH	Sodium hydroxide
FBCA	Fuzzy-ball coating agent
FBFA	Fuzzy-ball floss agent
FBKA	Fuzzy-ball core agent
FBMA	Fuzzy-ball membrane agent
HTHP	High temperature and high pressure
PV	Plastic viscosity
YP	Yield point
TS	Threshold stress
IP	Individual permeability
OP	Overall permeability
IIF	Individual instantaneous flow rate
OIF	Overall instantaneous flow rate
C	Coal
S	Sandstone
LS	Lower Shanxi Formation
LT	Lower Taiyuan Formation
UT	Upper Taiyuan Formation
US	Upper Shihezi Formation
N/M	Not measurable

References

Al-Ajmi, A., Al-Rushoud, A., Gohain, A., Khatib, F.I., Al-Gharib, M., Al-Ajmi, A., Al-Mekhlef, A.M., Mustafa, M.A.H., Mago, A., 2017. Drilling and completion fluids customization to achieve maximum well productivity in lower Burgan reservoir, case study from Kuwait field. In: Society of Petroleum Engineers-SPE/IATMI Asia Pacific Oil and Gas Conference and Exhibition. Jakarta, Indonesia. https://doi.org/10.2118/187025-MS.

Awan, F.U.R., Keshavarz, A., Akhondzadeh, H., Al-Anssari, S., Al-Yaseri, A., Nosrati, A., Ali, M., Iglauer, S., 2020. Stable dispersion of coal fines during hydraulic fracturing flowback in coal seam gas reservoirs-an experimental study. Energy Fuel. 34 (5), 5566–5577. https://doi.org/10.1021/ACS.ENERGYFUELS.0C00045.

Bai, Y., 2019. A new quantitative evaluation method for development area selection of tight gas and CBM commingled production. Nat. Gas. Ind. B 6 (2), 103–108. https://doi.org/10.1016/J.NGIB.2018.09.001.

Bourg, I.C., Ajo-Franklin, J.B., 2017. Clay, water, and salt: controls on the permeability of fine-grained sedimentary rocks. Acc. Chem. Res. 50 (9), 2067–2074. https://doi.org/10.1021/ACS.ACCOUNTS.7B00261.

Byrne, M.T., Patey, I.T.M., Twynam, A.J., 2000. A laboratory drilling mud overbalance formation damage study utilising cryogenic SEM techniques. Proceedings - SPE International Symposium on Formation Damage Control 295–303. https://doi.org/10.2118/58738-MS.

Chagneau, A., Claret, F., Enzmann, F., Kersten, M., Heck, S., Madé, B., Schäfer, T., 2015. Mineral precipitation-induced porosity reduction and its effect on transport parameters in diffusion-controlled porous media. Geochem. Trans. 16 (1), 1–16. https://doi.org/10.1186/S12932-015-0027-Z.

Chen, M., Zhao, H., Fang, H., Zhang, Y., 2017. Cross-sectional information on pore structure and element distribution of sediment particles by SEM and EDS. Scanning, 9876935. https://doi.org/10.1155/2017/9876935.

Chima, P., Baiyegunhi, C., Liu, K., Gwavava, O., 2018. Diagenesis and rock properties of sandstones from the stormberg group, karoo supergroup in the eastern cape province of South Africa. Open Geosci. 10 (1), 740–771. https://doi.org/10.1515/GEO-2018-0059.

Civan, F., 2007. Formation damage mechanisms and their phenomenological modeling- an overview. In: Society of Petroleum Engineers - European Formation Damage Conference. Scheveningen, Netherlands. https://doi.org/10.2118/107857-MS.

Dang, W., Zhang, H., Ye, C., Zhang, N., Li, Y., 2022. Research on damage prevention drilling fluid of hutubi built in low pressure and water-sensitive reservoir. J. Petrochem. Univ. 35 (1), 75–80. https://doi.org/10.3969/j.issn.1006-396X.2022.01.012 (in Chinese).

de Assumpcão Pereira-da-Silva, M., Ferri, F.A., 2017. Scanning electron microscopy. Nanocharacterization Techniques 1–35. https://doi.org/10.1016/B978-0-323-49778-7.00001-1.

Ding, J., Yan, C., He, Y., Wang, C., 2019. Secondary formation damage of low-pressure

layer during commingled production in multilayered tight gas reservoirs. Sci. Rep. 9 (1), 1–11. https://doi.org/10.1038/s41598-019-53940-6.
Guo, X., Xu, P., Xu, M., Cai, J., Huang, T., He, M., 2020. Formation protection method of oil-based drilling fluid for deep fractured tight gas reservoir. Energy Sci. Eng. 8 (10), 3682–3701. https://doi.org/10.1002/ESE3.775.
Halim, M.C., Hamidi, H., Akisanya, A.R., 2021. Minimizing formation damage in drilling operations: a critical point for optimizing productivity in sandstone reservoirs intercalated with clay. Energies 15 (1), 162. https://doi.org/10.3390/EN15010162.
He, J., Okere, C.J., Su, G., Hu, P., Zhang, L., Xiong, W., Li, Z., 2021. Formation damage mitigation mechanism for coalbed methane wells via refracturing with Fuzzy-Ball fluid as temporary blocking agents. J. Nat. Gas Sci. Eng. 90, 103956. https://doi.org/10.1016/J.JNGSE.2021.103956.
Huang, C., Zhao, F., Yuan, J., Wu, L., Chen, G., 2015. The characteristics of dolomite reservoir in saline lacustrine Basin, Qaidam, China. Carbonates Evaporites 31 (3), 307–317. https://doi.org/10.1007/S13146-015-0267-0.
Huang, Y., Cheng, S., Yu, H., He, Y., Lin, B., Feng, N., 2017. A semi analytical approach to estimate fracture closure and formation damage of vertically fractured wells in tight gas reservoir. J. Petrol. Sci. Eng. 150, 85–90. https://doi.org/10.1016/J.PETROL.2016.10.049.
Huang, C., Yuan, X., Song, C., Yuan, J., Ni, X., Ma, X., Zhang, S., 2018. Characteristics, origin, and role of salt minerals in the process of hydrocarbon accumulation in the saline lacustrine basin of the Yingxi Area, Qaidam, China. Carbonates Evaporites 33 (3), 431–446. https://doi.org/10.1007/S13146-017-0350-9.
Katende, A., Sagala, F., 2019. A critical review of low salinity water flooding: mechanism, laboratory and field application. J. Mol. Liq. 278, 627–649. https://doi.org/10.1016/J.MOLLIQ.2019.01.037.
Kumar, T., Todd, A.C., 1988. A new approach for mathematical modeling of formation damage due to invasion of solid suspensions. In: Society of Petroleum Engineers-SPE Annual Technical Conference and Exhibition. Houston, Texas. https://doi.org/10.2118/18203-MS.
Larestani, A., Mousavi, S.P., Hadavimoghaddam, F., Hemmati-Sarapardeh, A., 2022. Predicting formation damage of oil fields due to mineral scaling during water-flooding operations: gradient boosting decision tree and cascade-forward back-propagation network. J. Petrol. Sci. Eng. 208, 109315. https://doi.org/10.1016/J.PETROL.2021.109315.
Liang, T., Gu, F., Yao, E., Zhang, L., Yang, K., Liu, G., Zhou, F., 2017. Formation damage due to drilling and fracturing fluids and its solution for tight naturally fractured sandstone reservoirs. Geofluids 2017, 9350967. https://doi.org/10.1155/2017/9350967.
Lin, Z., Huang, J., Ma, C., 2017. Synthesis and performance of cationic plugging agent used in water-based drilling fluid. Journal of Liaoning Petrochemical University 37 (4), 11–14. https://doi.org/10.3969/j.issn.1672-6952.2017.04.003 (in Chinese).
Lin, C., Kang, Y., Xu, C., You, L., Zhang, Z., Tan, Q., 2020. An engineered formation-damage-control drill-In fluid technology for deep-fractured tight-sandstone oil reservoir in northern Tarim Basin. SPE Drill. Complet. 35 (1), 26–37. https://doi.org/10.2118/198915-PA.
Liu, H., Su, G., Okere, C.J., Li, G., Wang, X., Cai, Y., Wu, T., Zheng, L., 2022. Working fluid-induced formation damage evaluation for commingled production of multi-layer natural gas reservoirs with flow rate method. Energy 239, 122107. https://doi.org/10.1016/J.ENERGY.2021.122107.
Okere, C.J., Su, G., Zheng, L., Cai, Y., Li, Z., Liu, H., 2020. Experimental, algorithmic, and theoretical analyses for selecting an optimal laboratory method to evaluate working fluid damage in coal bed methane reservoirs. Fuel 282 (15), 1–8. https://doi.org/10.1016/j.fuel.2020.118513.
Potysz, A., Bartz, W., 2022. Bioweathering of minerals and dissolution assessment by experimental simulations—implications for sandstone rocks: a review. Construct. Build. Mater. 316, 125862. https://doi.org/10.1016/J.CONBUILDMAT.2021.125862.
Scimeca, M., Bischetti, S., Lamsira, H.K., Bonfiglio, R., Bonanno, E., 2018. Energy Dispersive X-ray (EDX) microanalysis: a powerful tool in biomedical research and diagnosis. Eur. J. Histochem. 62 (1), 89–99. https://doi.org/10.4081/EJH.2018.2841.
Shafiq, M.U., Mahmud, H.B., 2017. Sandstone matrix acidizing knowledge and future development. J. Pet. Explor. Prod. Technol. 7 (4), 1205–1216. https://doi.org/10.1007/S13202-017-0314-6.
Sokolov, S.A., Kelm, E.A., Milovanov, R.A., Abdullaev, D.A., Sidorov, L.N., 2016. Non-destructive determination of thickness of the dielectric layers using EDX. In: Society of Photo-Optical Instrumentation Engineers - SPIE International Conference on Micro- and Nano-Electronics, Zvenigorod, Russia. https://doi.org/10.1117/12.2265570.
Sui, W., Zhu, D., 2012. Determining multilayer formation properties from transient temperature and pressure measurements in gas wells with commingled zones. J. Nat. Gas Sci. Eng. 9, 60–72. https://doi.org/10.1016/J.JNGSE.2012.05.010.
Tan, Q., You, L., Kang, Y., Xu, C., 2021. Formation damage mechanisms in tight carbonate reservoirs: the typical illustrations in Qaidam Basin and Sichuan Basin, China. J. Nat. Gas Sci. Eng. 95, 104193. https://doi.org/10.1016/J.JNGSE.2021.104193.
Tao, X., Okere, C.J., Su, G., Zheng, L., 2022. Experimental and theoretical evaluation of interlayer interference in multi-layer commingled gas production of tight gas reservoirs. J. Petrol. Sci. Eng. 208, 109731. https://doi.org/10.1016/J.PETROL.2021.109731.
Ur Rahman Awan, F., Keshavarz, A., Akhondzadeh, H., Nosrati, A., Al-Anssari, S., Iglauer, S., 2019. Optimizing the dispersion of coal fines using sodium dodecyl benzene sulfonate. In: Society of Petroleum Engineers - SPE/AAPG/SEG Asia Pacific Unconventional Resources Technology Conference. Brisbane, Australia. https://doi.org/10.15530/AP-URTEC-2019-198250.
Wang, J., Zheng, L., Zhang, Y., Deng, J., Zhang, R., 2016. Piston-like plugging of fuzzy-ball workover fluids for controlling and killing lost circulation of gas wells. Nat. Gas. Ind. B3 (1), 77–81. https://doi.org/10.1016/J.NGIB.2015.12.011.
Wang, L., Yang, S., Peng, X., Deng, H., Meng, Z., Qian, K., Wang, Z., Lei, H., 2018. An improved visual investigation on gas–water flow characteristics and trapped gas formation mechanism of fracture–cavity carbonate gas reservoir. J. Nat. Gas Sci. Eng. 49, 213–226. https://doi.org/10.1016/J.JNGSE.2017.11.010.
Wang, Z., Qiu, Y., Guo, P., Du, J., Liu, H., Hu, Y., Zeng, F., 2019. Experimental investigation of the damage mechanisms of drilling mud in fractured tight gas reservoir. J. Energy Resour. Technol. 141 (9), 092907. https://doi.org/10.1115/1.4043247.
Wei, P., Zheng, L., Yang, M., Chen, Y., 2018. The application of fuzzy-ball drilling fluid to deepwater drilling to deal with highly mineralized formation brines and low-temperature environment. In: Proceedings of the International Conference on Offshore Mechanics and Arctic Engineering. Madrid, Spain. https://doi.org/10.1115/OMAE2018-78518.
Wei, P., Zheng, L., Yang, M., Wang, C., Chang, Q., Zhang, W., 2020. Fuzzy-ball fluid self-selective profile control for enhanced oil recovery in heterogeneous reservoirs: the techniques and the mechanisms. Fuel 275, 117959. https://doi.org/10.1016/J.FUEL.2020.117959.
Wetzel, M., Kempka, T., Kühn, M., 2020. Hydraulic and mechanical impacts of pore space alterations within a sandstone quantified by a flow velocity-dependent precipitation approach. Materials 13 (14), 3100. https://doi.org/10.3390/MA13143100.
Wuyep, E.O., Oluyemi, G.F., Yates, K., Akisanya, A.R., 2020. Evaluation of interactions between oilfield chemicals and reservoir rocks. Nat. Resour. Res. 29 (2), 1239–1258. https://doi.org/10.1007/S11053-019-09523-3.
Yang, G., Honglan, Z., He, L., Jianwen, Y., Qinghai, Y., Fuchao, S., 2013. Technique of water control and oil recovery based on water plugging combined with fracturing in low permeability and high water cut oilfield. In: Society of Petroleum Engineers-SPE Asia Pacific Oil and Gas Conference and Exhibition, Jakarta, Indonesia. https://doi.org/10.2118/165863-MS.
Yang, C., Tang, Y., Kang, H., Gou, M., Yu, X., 2021. Occurrence of minerals in coal and its geological controlling factors—significance in evaluation of coal washability. ACS Omega 6 (38), 24362–24376. https://doi.org/10.1021/ACSOMEGA.1C02522.
Yuan, B., Wood, D.A., 2018. A comprehensive review of formation damage during enhanced oil recovery. J. Petrol. Sci. Eng. 167, 287–299. https://doi.org/10.1016/J.PETROL.2018.04.018.
Zhang, Y., Su, G., Zheng, L., Liu, D., Guo, Z., Wei, P., 2019. The environmental friendliness of fuzzy-ball drilling fluids during their entire life-cycles for fragile ecosystems in coalbed methane well plants. J. Hazard Mater. 364, 396–405. https://doi.org/10.1016/J.JHAZMAT.2018.10.021.
Zheng, L.H., Kong, L., Cao, Y., Wang, H., Han, Z., 2012. A new fuzzy ball working fluid for plugging lost circulation paths in depleted reservoirs. Petrol. Sci. Technol. 30 (24), 2517–2530. https://doi.org/10.1080/10916461003792286.
Zheng, L., Chen, B., Zheng, Z., Tang, J., Hao, S., 2016. Anti-collapse mechanism of the cbm fuzzy-ball drilling fluid. Nat. Gas. Ind. B 3 (2), 152–157. https://doi.org/10.1016/j.ngib.2016.03.011.
Zheng, L., Wei, P., Zhang, Z., Nie, S., Lou, X., Cui, K., Fu, Y., 2017. Joint exploration and development: a self-salvation road to sustainable development of unconventional oil and gas resources. Nat. Gas. Ind. B 4 (6), 477–490. https://doi.org/10.1016/j.ngib.2017.09.010.
Zheng, L., Su, G., Li, Z., Peng, R., Wang, L., Wei, P., Han, S., 2018. The wellbore instability control mechanism of fuzzy ball drilling fluids for coal bed methane wells via bonding formation. J. Nat. Gas Sci. Eng. 56, 107–120. https://doi.org/10.1016/j.JNGSE.2018.05.008.
Zheng, L., Tao, X., Wei, P., Wu, T., Liu, H., Cao, Z., 2021. Multi-reservoir production damage physical simulation system and its application in coal-measure gas production. J. China Coal Soc. 46 (8), 2501–2509. https://doi.org/10.13225/j.cnki.jccs.CB21.0808 (in Chinese).
Zhu, Q., Wang, Y., Zhang, Y., Wang, Z., Liu, C., 2018. Successful applications of a novel compound lost circulation additive with variable structure. In: Society of Petroleum Engineers - SPE Kingdom of Saudi Arabia Annual Technical Symposium and Exhibition. Dammam, Saudi Arabia. https://doi.org/10.2118/192403-MS.